Single Molecule Imaging of Proteins That Recognize and Repair DNA Damages

Yupeng Qiu and Sua Myong

(Invited Paper)

***Abstract*—Double-stranded DNA breaks are common cytotoxic lesions that can be repaired by several well-known repair pathways. One of the most prominent repair strategies is homologous recombination (HR). Over the years, HR has been studied primarily through biochemical analysis. However, recent advances in single molecule techniques have enabled researchers to investigate the repair mechanisms at the single protein level, with nanometer resolution and millisecond time scale. The ability to fluorescently label different regions of the protein or protein complex allows real-time monitoring of conformational changes, as well as detailed mechanisms with which the proteins target DNA damage and conduct repair. Here, we review some recent single molecule studies that provide new insights into the molecular mechanisms involved in mismatch and homologous repair of DNA.**

***Index Terms*—DNA mismatch repair, DNA double strand break, homologous recombination, single molecule imaging.**

I. Introduction

IF LEFT unchecked, DNA damage in bacteria and eukaryotic cells can lead to harmful mutations of genetic information which encodes many vital cell functions [1], [2] and induces many types of cancers [3]–[7]. This genomic instability can arise from errors that occur during DNA replication. Postreplicative base mismatches or short insertion errors in DNA are repaired by a system of mismatch repair (MMR) proteins [8]–[10], such as MutSα and MutLα.

UV irradiation and chemical damage commonly induce another form of damage—double-stranded DNA breaks (DSBs). Primarily, DSBs are repaired by the homologous recombination (HR) pathway, which is mediated by the Rad51 recombinase in eukaryotes [11], [12] and its homolog RecA in bacteria [13].

Previous biochemical studies have demonstrated the importance of these proteins in their respective repair pathways. However, the specific mechanisms by which the repair proteins target and localize the DNA damage sites remain elusive. Recent developments in high-resolution single molecule techniques have enabled the high precision monitoring of individual molecules in real time. Included in this review are some of the most recent advances made in the imaging of DNA repair proteins using various single molecule techniques, as well as some perspectives on the future of this area of research.

Manuscript received June 14, 2013; revised September 9, 2013; accepted September 9, 2013. This work was supported in part by the U.S. Department of Commerce under Grant BS123456.

The authors are with the Department of Bioengineering, University of Illinois, Champaign, IL 61820 USA (e-mail: yqiu2@illinois.edu; smyong@illinois.edu).

Color versions of one or more of the figures in this paper are available online at http://ieeexplore.ieee.org.

Digital Object Identifier 10.1109/JSTQE.2013.2284430

II. Finding Small Errors in DNA

A. Post-Replicative Mismatch Repair

In MMR, the biggest challenge faced by the proteins is quickly locating the site of DNA damage out of the sea of normal DNA, and recruiting accessory factors to initiate the repair complex. In eukaryotic cells, these functions are performed by MutSα and MutLα protein complexes, which are highly conserved among many species. It was observed that the target association rates of these protein complexes far exceed (several orders of magnitude faster) what could be achieved with simple 3-D diffusion, and several mathematical models introduced a concept collectively referred to as "facilitated diffusion" to explain this phenomenon [14], [15]. Previous single-molecule studies have demonstrated that the protein complex is able to undergo 1-D sliding and hopping for facilitated diffusion on undamaged DNA [16], [17]. A recent study by Gorman *et al*. [18] revealed that MutSα first targets a DNA mismatch through a combination of 3-D diffusion and ATP-dependent 1-D sliding, followed by MutLα searching and locating the lesion-bound MutSα via 3-D diffusion and 1-D hopping. When complexed, MutSα/MutLα also scans the DNA flanking the mismatch via 1-D sliding.

Gorman *et al*. used nanofabricated DNA curtains, imaged by total internal reflection fluorescence microscopy (TIRFM), to observe the interactions between MutSα, MutLα and mismatch-containing DNA substrates. They demonstrated how each protein was able to conduct their respective target searches individually and collaboratively throughout the early stages of MMR [18]. Double-tethered DNA curtains were constructed by anchoring one end of the λ-DNA (with specifically engineered G/T mismatches, labeled MM) onto a lipid bilayer on the surface of a microfluidic sample chamber and the other end to a digoxigenin-antibody linkage. Then, hydrodynamic forces stretched the DNA into alignment with nanofabricated barriers [see Fig. 1(a)]. MutSα and MutLα proteins were labeled with QDs, and TIRFM was used to visualize the binding of molecules [see Fig. 1(b)].

Once MutSα was injected into the sample chamber, flow was terminated and the protein began searching the DNA for mismatches. Real-time tracking of the protein trajectories suggest that MutSα located the mismatches either through 1-D sliding

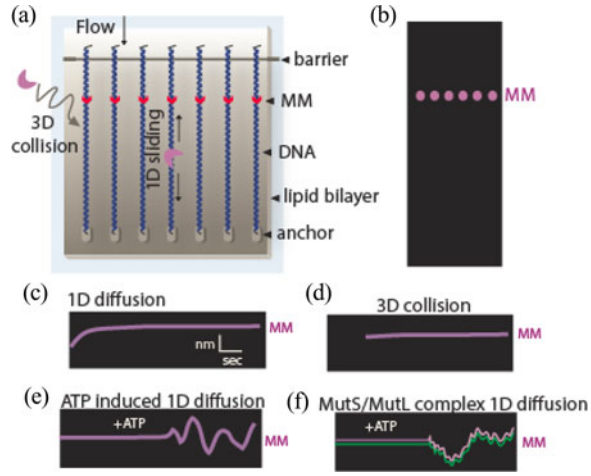

Fig. 1. Mismatch recognition by MutSα and Mutlα. (a) Schematic of the double-tethered DNA curtains. (b) Proteins labeled with QDs and visualized using TIRFM. (c)–(f) Example of MutSa/MutL sliding in search of the MM.

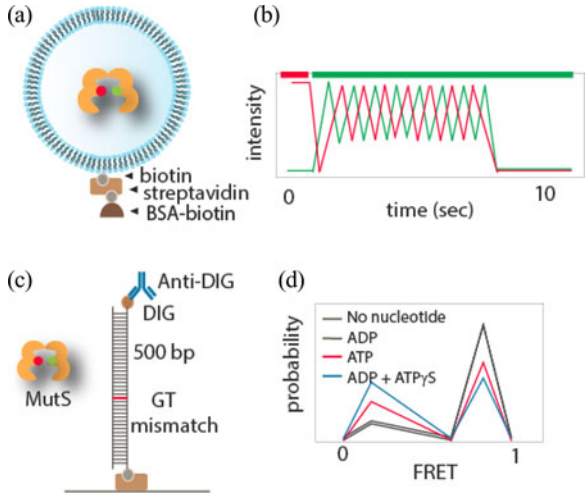

Fig. 2. Large conformational changes in Taq MutS by smFRET. (a) Surface immobilization using liposome encapsulation. (b) Example of a single molecule trace. (c) Surface tethered DNA and doubly labeled MutS. (d) Histogram analysis of MutS conformation in different ATP analogs.

(42.5% of observed events) [see Fig. 1(c)] or 3-D collision (57.5% of observed events) [see Fig. 1(d)]. Upon injection of ATP into the chamber, a majority of the MutSα (85%) dissociated from the mismatches and began scanning the flanking DNA through 1D diffusion—no longer targeting the mismatch [see Fig. 1(e)]. This is likely due to the absence of an obligatory rotational component as shown previously [19]. When adding QD-tagged MutLα to mismatch-bound MutSα, MutLα colocalized to MutSα via 3-D diffusion (45% of observed events) and 1-D hopping (55% of observed events) and the complex remained bound at the lesion in absence of ATP. After the addition of ATP, MutSα/MutLα was released from the bound lesion and began scanning the flanking DNA by 1-D diffusion as a stable complex [see Fig. 1(f)].

Real-time observation of protein–DNA interaction to locate the target site led them to consider various modes of diffusion to understand how mismatch can be targeted through facilitated diffusion, during the early stages of MMR. ATP-induced release of MutS indicates a possible mechanism of the MSH protein to avoid rebinding the same mismatch while searching the DNA strands [18].

Another recent study investigated further into conformational changes in MutS as it targets DNA mismatches and initiates repair signaling [20]. Qiu and Weninger employed single-molecule Förster resonance energy transfer (smFRET) by specifically labeling MutS dimer units with fluorescent dyes (FRET pair, Cy3 as donor and Cy5 as acceptor). FRET was measured in the presence and absence of ATP and mismatched DNA [21]. The doubly labeled MutS was encapsulated in a liposome for observing single molecules of MutS without having to surface-immobilize the protein. Instead, the liposome was immobilized to the surface through a biotin-streptavidin linkage [see Fig. 2(a)]. Single-molecule traces show that MutS, in the absence of DNA, undergoes FRET fluctuation, demonstrating inherent conformational dynamics of the protein dimer [see Fig. 2(b)].

When the dual-labeled MutS dimer is added to a surface-immobilized, end-blocked, 500 bp DNA strand with G/T mismatch [see Fig. 2(c)], the FRET fluctuations stabilize at the high FRET ($E_{\mathrm{corr}} \sim 0.94$) MutS conformation. The same pattern is observed in the presence of ADP. In contrast, with the addition of ATP and its non-hydrolyzable analog, ATPgS, the high FRET peak diminishes ($E_{\mathrm{corr}} \sim 0.88$) and a low FRET peak ($E_{\mathrm{corr}} \sim 0.2$) emerges [see Fig. 2(d)]. The appearance of the low FRET peak is only seen when the end of the DNA is blocked with anti-Dig, suggesting that the subunits may function in the form of a sliding clamp. In the case of unblocked DNA, the sliding clamp will simply slide off of the DNA. Formation of a sliding clamp was further confirmed using a donor-labeled MutS dimer with a surface-immobilized, 500 bp, end-blocked DNA, which was labeled with an acceptor dye positioned 9 bps away from a G/T mismatch. With addition of ADP, MutS bound to the mismatch site, resulting in a FRET efficiency of ~ 0.6. By exchanging the ADP with ATP or ATPγS, the 0.6 FRET state disappears, indicating that the clamp slides away from the mismatch site.

To track the conformational changes within the MutS dimer while undergoing mismatch recognition, FRET was measured from the dual-labeled MutS dimers interacting with the G/T mismatched DNA. 3 distinct FRET states were shown as the MutS binds to the mismatch ($E_{\mathrm{corr}} \sim 0.94$), followed by a conversion to an intermediate state ($E_{\mathrm{corr}} \sim 0.65$), then to the sliding clamp state ($E_{\mathrm{corr}} \sim 0.2$). The corresponding dwell times revealed the intermediate conformation persisting for seconds, which may allow enough time to interact with downstream proteins required for repair.

III. HR Repair for DSBs

A. RecA and Homology-Directed DNA Repair

HR is one of the most common DSB repair pathways [22]. A blunt-end DSB is resected to expose a single-stranded DNA (ssDNA) tail, which is coated by the RecA recombinase

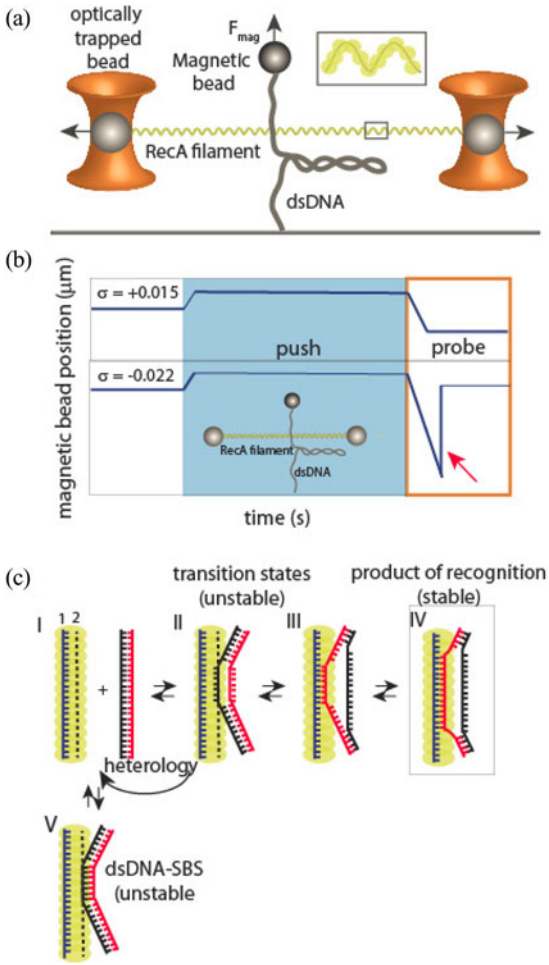

Fig. 3. Mechanism of homology recognition of RecA in DNA recombination probed with dual- molecule assay. (a) Dual-molecule assay. (b) Push-probe experiments. (c) Mechanistic model for RecA (shown in green) homology search and recognition.

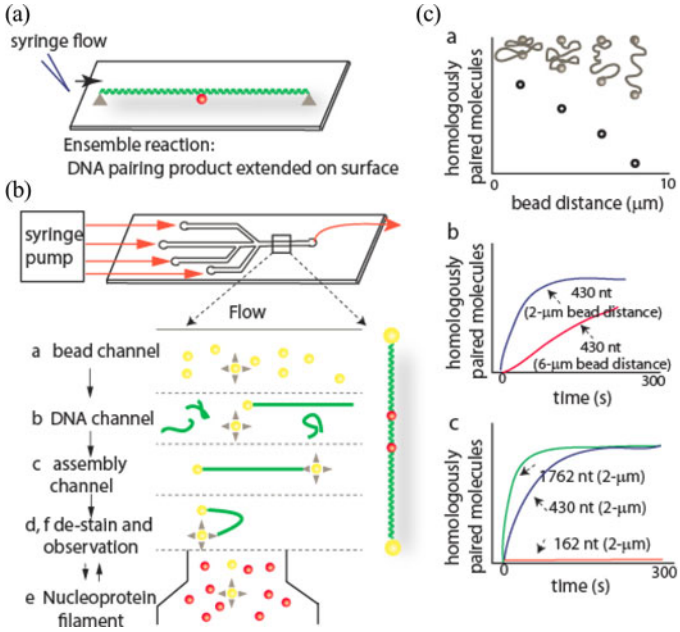

Fig. 4. RecA filament conducts 3-D homology search. (a) Experimental schematics. (b) Four-channel flowcell with DNA dumbbell assembly and RecA pairing reaction. (c) Analysis of homologous pairing dependent on bead to distance.

protein in *E. coli* and Rad51 in yeast and humans. Upon filament formation, the presynaptic complex searches neighboring DNA to find a matching sequence for strand exchange. The filament formed by RecA is able to localize a homologous sequence with remarkable speed and fidelity, despite a large population of DNA molecules.

Vlaminck *et al*. used a dual-molecule manipulation technique in order to study RecA–DNA binding interactions with the focus of determining whether or not a secondary DNA-binding site (SBS) on RecA can lead to quick homology recognition [23]. Using a combination of single-molecule magnetic-tweezers and optical-tweezers, a RecA filament-covered DNA strand (held in place with optical tweezers) is brought into contact with single-stranded DNA (ssDNA) or a coiled, double-stranded DNA (ds-DNA) tethered with magnetic tweezers. On this platform, the strength and frequency of binding interactions were measured [see Fig. 3(a)] [24]. Since the negative supercoiling of dsDNA was known to promote the frequency of occurrence [27], it was tested if this phenomenon can also enhance the probability of homology recognition. The RecA filament is assembled onto a 20 kb ssDNA, which is mechanically stretched by optical tweezers and brought into contact with a homologous dsDNA, tethered to and rotated by magnetic tweezers. The result showed a remarkably strong affinity of RecA binding to the negatively supercoiled dsDNA and the lack of binding to positively supercoiled dsDNA [see Fig. 3(b)], indicating that even the smallest underwinding of the dsDNA can encourage the joint-molecule formation [23]. This implies the designated role of SBS in solely interacting with one strand of the incoming dsDNA during homology sampling [see Fig. 3(c)]. This functionality allows RecA to quickly pass over non-homologous strands during the homology search [25], [26].

This phenomenon points to a model where homologous recognition probability is greatly enhanced when the donor DNA exhibits spontaneous DNA-breathing dynamics [28].

The question of how a RecA filament locates the homologous target in dsDNA was addressed by Forget and Kowalczykowski [29]. In a microfluidic chamber, fluorescently labeled λ-DNA was stretched by flow and immobilized by having both ends biotinylated. The DNA was extended to nearly B-form length. The addition of fully homologous fluorescent ssDNA produced DNA pairing products at the homologous regions on the λ-DNA [see Fig. 4(a)]. Pre-formed fluorescent RecA filament was then introduced into the flow cell with λ-DNA and the buffer flow stopped. The real-time observation revealed the lack of any interactions between the filament and the double-tethered dsDNA. However, some singly tethered dsDNA revealed a stable pairing product, suggesting that a free DNA end or a randomly coiled DNA was needed for pairing. In addition, the λ-DNA with both ends attached on the same side of the flow channel also showed evidence of homologous pairing, suggesting that a free end of the DNA was not required,

rather that the homology search required the 3-D states which became accessible when the DNA was randomly coiled up [29].

To investigate this, an alternative single molecule technique was setup using a specialized flowcell [see Fig. 4(b)] which uses two optical laser traps operating in position-clamp mode and epi-fluorescent imaging as the detection method. A λ-DNA attached to two beads via biotin-streptavidin (dumbbell) is held in place by the dual-optical traps [see Fig. 4(b.a–c)]. Once trapped, it was de-stained [see Fig. 4(b.d)] before being added to the nucleoprotein filament reservoir which contains fluorescent ssDNA-RecA filaments in a flow-free reservoir [see Fig. 4(b.e)]. The DNA is then pulled back to the de-staining chamber and examined for DNA pairing products [see Fig. 4(b.f)]. After a 2 min incubation, 90% of the dsDNA molecules were found stably bound to RecA filament [see Fig. 4(c.a)]. The beads are then separated via dual-optical trap manipulation [see Fig. 4(c.a)] to determine the effect of the 3-D conformation of DNA (end-to-end distance) on the RecA-mediated DNA pairing reaction. As the beads are separated further apart (2 um to 6 um), the homologous pairing rate decreases from 0.023 to 0.0056 s^{-1} [see Fig. 4(c.b)], indicating that the pairing rate was dependent on dsDNA conformation and was not sequence-specific. When the length of the RecA filament was varied, the pairing rate also decreased with shorter length, until a threshold length is reached where no stable RecA filaments form [see Fig. 4(c.c)].

This study established that both the 3-D conformation of dsDNA and the length of the RecA filament are rate-limiting factors for DNA homologous pairing. Based on their findings, the authors propose a model termed "intersegmental contact sampling" [29], where the 3-D conformation of dsDNA allows RecA filament to come into brief contacts with multiple segments of the dsDNA to facilitate the homology search.

The mechanism of RecA homology search after random 3-D collision is examined in great details in a study by Ragunathan and Ha. The authors employed smFRET-based assays to detect the interactions between RecA filament and non-homologous and homologous DNA. They show that RecA performs homology searches on DNA via rapid sliding to significantly shorten the search time [30].

First, the dynamic interaction between RecA filament and non-homologous dsDNA is probed by 2-color smFRET assay. A stable RecA filament is formed on the acceptor-labeled DNA. Here, a partially duplexed DNA is used as a recombination intermediate mimic (resected DNA). This DNA is immobilized to surface via biotin-strepatavidin linkage. Next, donor-labeled, non-homologous dsDNA is applied to the single molecule surface. FRET signal appears when the dsDNA pairs with the RecA filament [see Fig. 5(a)]. Single molecule traces show short bursts of rapid FRET fluctuation, indicating a DNA sliding as the possible mechanism by which RecA filament searches for homology [see Fig. 5(b)]. Can a RecA filament recognize a homologous sequence while sliding? To answer this question, the DNA substrate is changed to one that contains two matching homologous sites of different lengths located along the ssDNA. When the homology length is only 5nts, the search becomes erratic and gives results similar to those obtained from the non-homologous DNA search [see Fig. 5(c)]. As the

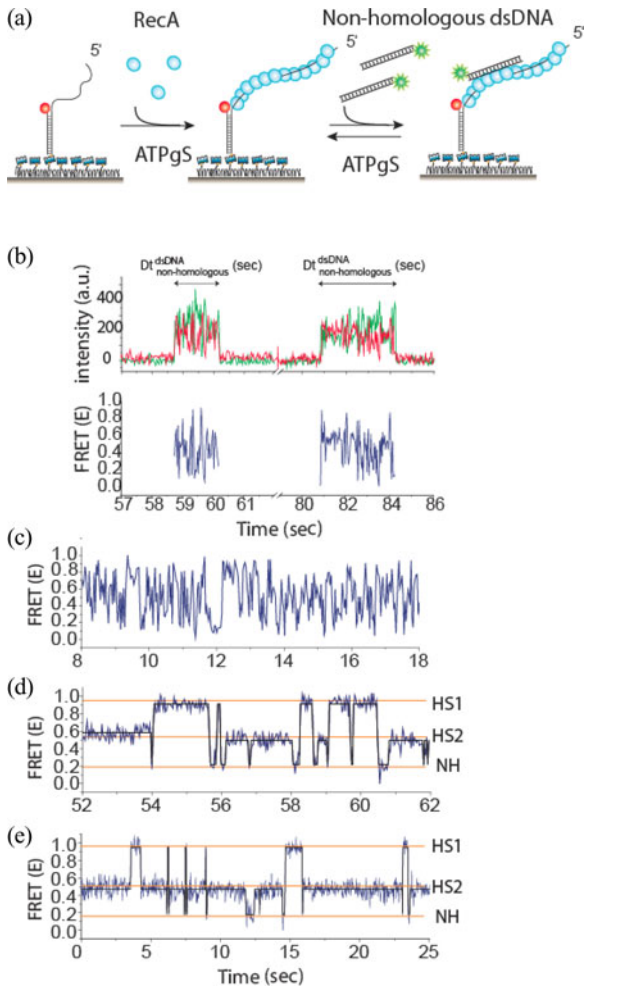

Fig. 5. RecA filament sliding on DNA facilitates homology search. (a) Schematic of smFRET assay of interactions. (b) Example single molecule trace showing rapid FRET fluctuations. (d) smFRET trace showing homology search when HS1 and HS2 are 5nts long. (e) smFRET trace showing homology search when HS1 and HS2 are 6nts long. (f) smFRET trace showing homology search when HS1 and HS2 are 7nts long.

homology length extends to 6 or 7 nts [see Fig. 5(d), and (e)], there are well distinguished pauses in the FRET traces where the FRET signal is stable, indicating an alignment of the homologous DNA segments. The exchange between two well distinguished FRET states clearly indicates the dynamic transition of RecA filament between the two homology sites.

This study demonstrates that the homology recognition for RecA-mediated search can occur while 1-D sliding for as few as 6 nts of complementary base pairs of DNA. The contact time is brief and a segment as short as 6 nts can significantly improve the recognition efficiency [30].

IV. Proteins That Aid During the HR Pathway

A. SSB Protein Diffuses on ssDNA Via Reptation

In addition to RecA and its homolog proteins (yeast Rad51, human Rad51), there are accessory proteins that enhance filament formation, primarily acting to reduce ssDNA distortions or to enhance binding affinity via extending the binding

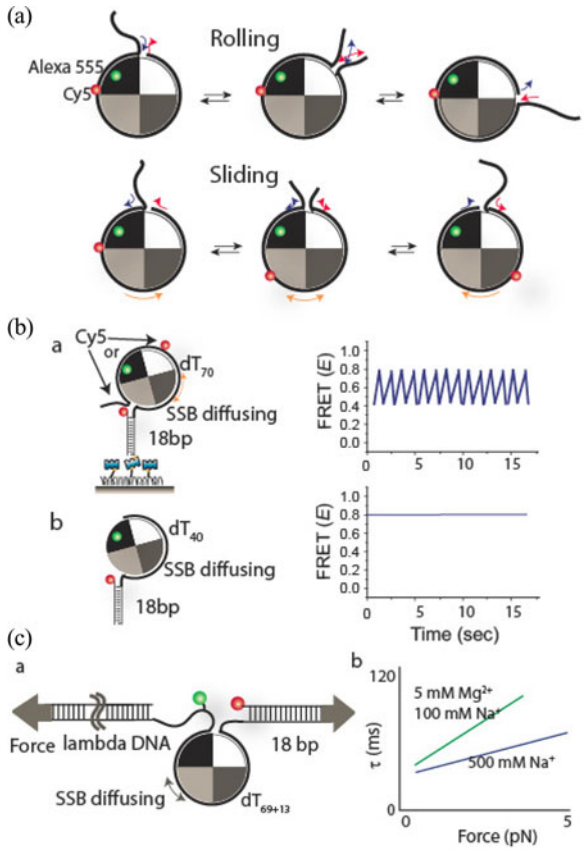

Fig. 6. SSB Functions as a Sliding Platform. (a) Schematic of rolling (upper) versus sliding (lower) mechanism. (b) Experimental schematics to distinguish between sliding and rolling and the single molecule FRET traces for each case. (c.a) FRET DNA with excess ssDNA tail length in order to form a DNA bulge under applied force. (c.b) Diffusion time under different ionic conditions.

contact [31]. SSB is one such protein, which binds to and controls the accessibility of ssDNA via diffusion along the ssDNA [32]. Furthermore, the diffusion can assist in the melting of DNA secondary structures, thereby stimulating RecA filament elongation [33]. For a protein with such a large binding size ($\sim$ 65 nts), how SSB is able to quickly diffuse on DNA remains unknown. A recent study by Zhou and Ha applied a newly developed technique that combines single molecule fluorescence and force spectroscopy [34] to probe the tension-dependent conformational changes between DNA and SSB protein [35]. They used λ-DNA, tethered to a bead held in an optical trap. Fluorescent probes were placed at various locations along the DNA and/or protein to probe their dynamic interaction.

Two possible mechanisms can account for the way SSB diffuses on DNA—rolling or sliding [36], [37]. In a rolling scheme, one end of the ssDNA unwraps from the SSB tetramer and the other end of the ssDNA rewraps around it, resulting in a 1-D walk of SSB on DNA. In a sliding scheme, the entire ssDNA "slides" on the protein surface [see Fig. 6(a)]. A series of sm-FRET experiments are performed to distinguish between these two mechanisms. The DNA construct has an acceptor attached to the end of $(dT)_{70}$ ssDNA or to the middle part of the ssDNA. Since the ssDNA tail length is sufficient for SSB binding, FRET fluctuations result for both the end-labeled and middle-labeled DNA, indicating that SSB is sliding [see Fig. 6(b.a)]. When tested on a ssDNA, $(dT)_{40,}$ which is shorter than the binding size of SSB, the FRET remains unchanged, also supporting the sliding model [see Fig. 6(b.b)].

Upon confirming that SSB diffuses by sliding, two possible mechanisms of sliding were considered. In one scheme, all contacts with the protein are broken and the protein slides to an adjacent position between the protein-DNA bonds reform, this is termed the "Sliding-Without-Bulge" model. The second scheme has a bulge present in the DNA that promotes the translocation of SSB tetramer, referred to as the "reptation" model. To differentiate between the two schemes, an experiment was conducted using a FRET DNA construct with excess ssDNA tail length (13 nts longer than the usual 69 nts ssDNA). Since a DNA bulge can be formed from the excess DNA under the right thermal conditions, an applied force is used to control the amount of excess ssDNA, hence the frequency of the DNA bulge formation. Since the reptation model favors protein diffusion via DNA bulge, increased tension on the DNA will slow down SSB diffusion, whereas the "sliding-without-bulge" model will show faster diffusion rate [see Fig. 6(c.a)]. Under constant force, SSB diffused along ssDNA under tension. However, when measuring the characteristic time scale for diffusion τ under different ionic conditions (100 mM Na^+ and 500 mM Na^+), it was found that the diffusion rate slowed down with increased applied force F in both cases. The difference in diffusion rate between the two ionic conditions is likely due to the change in persistence length of ssDNA under the influence of different salt conditions [38]. This result favors the reptation model as the primary SSB sliding mechanism on ssDNA.

B. Rad52 Phosphorylation Enhances ssDNA Binding and Annealing

Rad52 belongs to the RAD51 protein family. It plays an important role in HR repair by promoting the annealing of two complementary strands of RPA-coated ssDNA and mediating Rad51 filament formation, similar to the function of BRCA1-BRCA2 [39]. Honda and Spies looked at how the phosphorylation of Rad52 modulates its function in HR-directed repair [40]. c-ABL kinase targets tyrosine 104 (Y104pCMF), which is in a highly conserved region in the N-terminus of Rad52, and is known to facilitate the localization of Rad52 at the site of DNA damage [41]. Single-molecule FRET analysis using TIRFM was employed to examine whether the Y104pCMF phosphorylation of Rad52 promotes the protein's selective binding to ssDNA over dsDNA.

A gapped DNA substrate immobilized to a PEG-coated surface was used to examine the wild type and mutant Rad52 protein binding dynamics. The DNA substrate was dual-labeled with donor and acceptor fluorophores at the opposite ends of a 28 nts long ssDNA, both of which were connected to stretches of dsDNA [see Fig. 7(a)]. Prior to the addition of Rad52 protein, low FRET was observed. Upon binding of Rad52 protein, the Rad52 is expected to wrap around the ssDNA, yielding a high FRET signal. Representative FRET traces are shown in

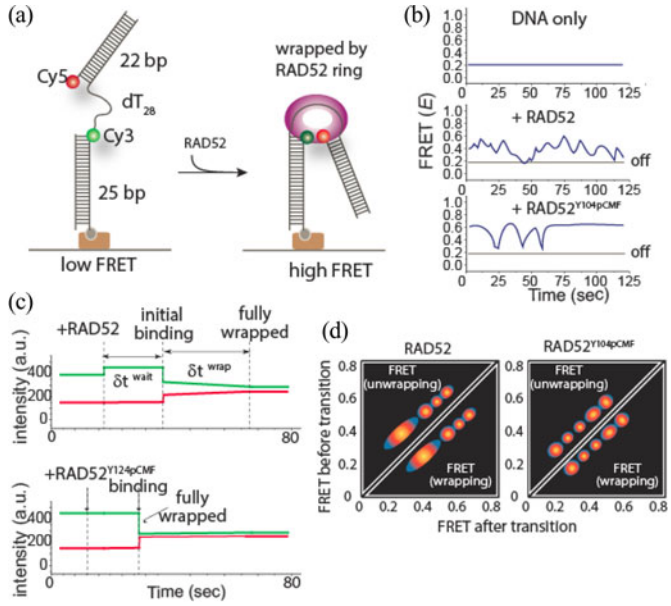

Fig. 7. Rad52 and mutant exhibit different DNA-binding dynamics. (a) Experimental schematic. (b) Example FRET traces. (c) Example intensity time traces showing the initial interactions. (d) Transition density plots.

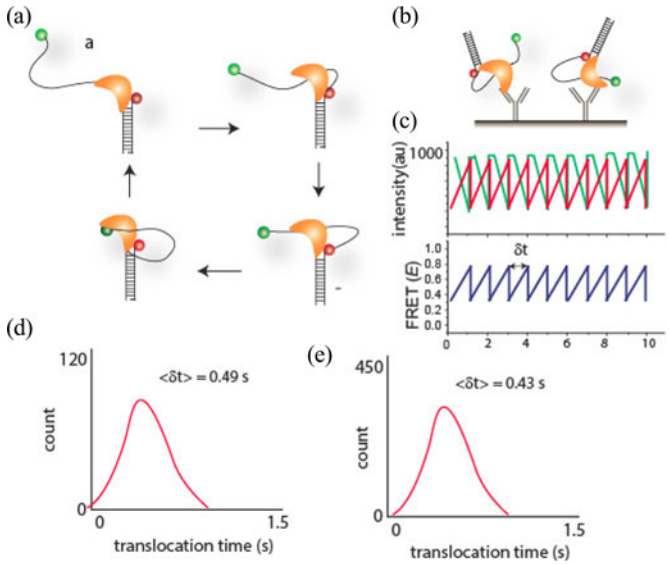

Fig. 8. Single Molecule pull-down (SimPull) on PcrA translocation. (a) Schematic of PcrA translocation on ssDNA. (b) Single molecule pull-down (SiMPull) experimental schematic. (c) Example of intensity and FRET traces. (d) Dwell time analysis which reveals single nucleotide translocation step.

Fig. 7(b), before and after 5 min of incubation with Rad52 and Rad52$^{\mathrm{Y104pCMF}}$.

The traces clearly show that the addition of Rad52 initiates the wrapping of the ssDNA region, bringing the two dyes closer together, resulting in the appearance of higher FRET signals.

To more clearly capture the initial binding and wrapping of ssDNA by Rad52 and Rad52$^{\mathrm{Y104pCMF}}$, the protein was injected into the reaction chamber while donor and acceptor signals were recorded. The changes in the signal intensities in Fig. 7(c) depict the different stages of DNA-protein interaction. Both traces begin with DNA-only intensities (i.e., low FRET). The Rad52$^{\mathrm{Y104pCMF}}$ shows a much shorter initial binding time than the wild type Rad52. To represent data from many molecules, 2000 FRET transitions were extracted from 50 single molecule FRET trajectories and plotted as 2-D transition density plots [see Fig. 7(d)] [42], [43]. The upper left half corresponds to the FRET values that represent states involved in unwrapping whereas, in the lower right half, the FRET transitions represent the DNA wrapping process. In both TDP analyses, five FRET transition peaks can be seen for the wrapping and unwrapping ssDNA, indicating the existence of six distinct FRET states. The discrete peaks shown on TDPs indicate that the overall DNA binding/releasing reaction by both Rad52 and Rad52 $^{\mathrm{Y104pCMF}}$ involves stepwise wrapping/unwrapping. In addition, the six FRET states for a 28 nts long ssDNA yield a stepsize of approximately 4 nts for Rad52 monomer [44]. The transition rates of wrapping and unwrapping of Rad52 and Rad52$^{\mathrm{Y104pCMF}}$ are shown in Fig. 7(c) and (d). As seen, the wild type Rad52-gapped DNA complex is the least stable at high FRET (ssDNA fully wrapped) while Rad52$^{\mathrm{Y104pCMF}}$-gapped DNA complex showed a much faster wrapping toward the high FRET state. This is likely due to the enhanced binding to ssDNA over dsDNA influenced by Y104 phosphorylation [40]. It is hypothesized that this allows the Rad52 to preferentially position itself to the resected ssDNA region for a DSB, and can aid in the quality control of homology search by ensuring that only the regions of substantial continuous complementarity are annealed [40].

V. Advancement in Single Molecule Techniques

A. SiMPull Allows for the Probing of Protein Complexes That Exists in Cell and In Vivo

One of the limitations of the single molecule technique is the inability to study proteins in physiologically relevant conditions. Often, DNA-protein and protein–protein interactions are studied in isolation by *in situ* preparation. Jain and Ha developed a novel technique that combines single-molecule detection and immunofluorescence assay, termed single-molecule pull-down (SiMPull). It enables the visualization of cellular protein complexes that naturally exist in cells [45]. As one of the potential applications of the SiMPull technique, the authors chose to pull down a well-characterized bacterial helicase, PcrA, from cell lysate. PcrA was previously studied by Park and Ha [46]. In this study, PcrA was shown to exhibit highly periodic and repetitive cycles of translocation on ssDNA. PcrA positions itself at the ss/dsDNA junction and reels in ssDNA in repetition [see Fig. 8(a)]. It was shown that such a repetitive activity efficiently dismantles RecA filaments and thereby negatively regulates DNA repair/recombination. In this regard, PcrA is an anti-recombinase. The same protein was pulled down directly from *e. coli* cells that overexpress PcrA for SiMPull experiments. When FRET-labeled, non-biotin DNA was applied [see Fig. 8(b)], the surface immobilized PcrA showed the identical repetitive motion described previously [see Fig. 8(c)]. The dwell time analysis performed by collecting times in between successive FRET peaks revealed a non-exponential distribution, indicating hidden substeps within one translocation cycle.

This data fitted to a Gamma-distribution function revealed a single nucleotide as the smallest elementary step of translocation (i.e., PcrA reels in ssDNA single nucleotide at a time) [see Fig. 8(d)] [46]. The same dwell time analysis, performed for the PcrA prepared by SiMPull, yielded the same distribution, clearly indicating the same protein activity resulting from both the purified PcrA and pull-down PcrA [see Fig. 8(e)].

Thus, SiMPull has demonstrated its advantage by eliminating the need for protein purification. Although it is not reviewed here, SiMPull offers a unique ability to probe the protein complex in its native context. For example, protein can be pulled down from cell lysate while being bound to its cofactor or as an oligomer. This platform enables quantitation of the stoichiometry of the protein by counting photobleaching steps of the GFP-fused proteins and determination of the presence of associated cofactors by immunofluorescence probing.

B. Study of Large Protein Complex With Many Subunits Working in Conjunction

Many proteins in cells exist as a large collection of subunits working in conjunction with each other. Often, these proteins require the presence of all or most subunit components for performing its function properly. The DNA polymerase III holoenzyme (Pol III HE) in the *Escherichia coli* replicase system contains at least 17 subunits with multiple $\alpha\varepsilon\theta$ cores, β_2 sliding clamps, and a $\delta\delta'\tau_3\psi\chi$ clamp loader assembly [47]. A recent study by Jergic and Van Oijen reported on the activity of the complex composed of $\alpha\varepsilon\theta$ and β_2 on primer-template DNA. The study focused on the question of how the interaction of the ε proofreading subunit with the β_2 subunit [48] is maintained in the polymerization mode of DNA synthesis. To test whether the ε–β interaction promotes the Pol III replicase in the polymerization mode, single molecule replication assays were set up by arranging λ-DNA between a glass surface and a 2.8 μm bead. The λ-DNA is extended by laminar buffer flow and fully loaded with the oligonucleotides as shown in Fig. 9(a). The position of the bead on the λ-DNA is tracked over time as the DNA shortens during replication. Trajectories of the bead shown in Fig. 9(b) reveal the rate, extent, and duration of the leading-strand synthesis. 61% of the molecules show long pauses ($\geq$ 3 sec) followed by further synthesis. The pauses reflect a situation where the template has no free 5' end and no replication origin [49], [50]. In this case, DnaB must remain bound at the fork while the replisomal component dissociates during the pause. Fig. 9(c) and (d) shows that the mean duration of these long pauses was inversely proportional to the concentration of $\alpha\varepsilon_{wt}\theta$, whereas processivity remained constant for both concentrations. This indicates that each pause signifies a new replication event, which is mediated by the core unit dissociation and re-association. For wildtype, $\alpha\varepsilon_{wt}\theta$, the rate of synthesis and the lifetime are estimated to be approximately 900 bps/s and 10 s, respectively [see Fig. 9(e) and (f)]. When the same parameters were measured for different constituents (i.e., replisomes containing α alone, or $\alpha\varepsilon\theta$ cores containing different ε–β interaction strength variations of ε), the processivity and rates increased as the ε–β interaction strength was increased, yet the lifetime remained constant at about 10 s

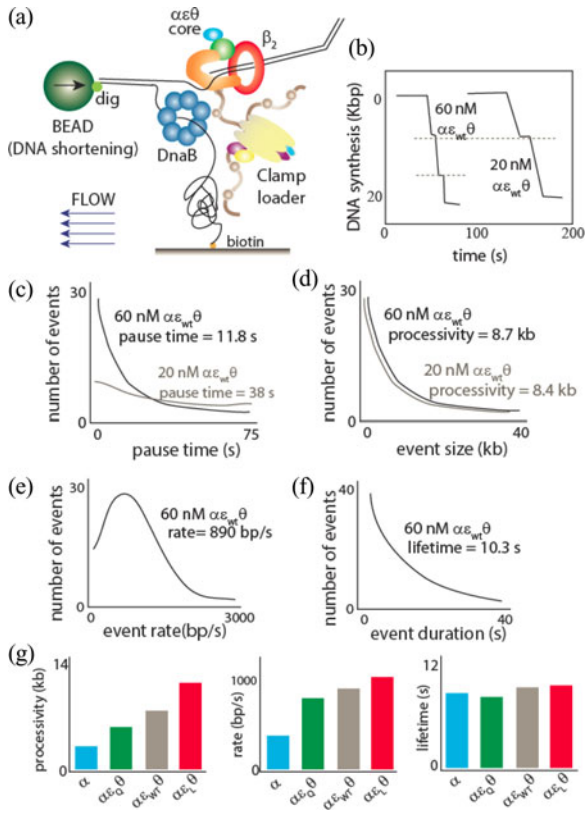

Fig. 9. Single molecule replication experimental schematic of single molecule DNA replication assay. (a) Experimental Schematic of single molecule DNA replication assay. (b) Example trajectories of bead position as replicaton proceeds for different concentration of protein complexes. (c) Distribution of pause time durations .(d) Distribution of processivity. (E) Distribution of the synthesis rate at 60 nM concentration. (f) Distribution of the lifetime. (g) Processivity, synthesis rate, and lifetime comparison.

[see Fig. 9(g)]. This shows the lifetime to be a common rate-limiting step in the dissociation of α-cores, and involves some kind of protein–protein or DNA–protein interactions that are much stronger than the ε–β interaction [51].

The proteins and protein complexes studied by SiMPull and the single molecule replication assays, which were presented in this section, do not pertain to DNA recombination or repair. However, they are included to demonstrate the potential usage of both techniques in the experimental stages where DNA-protein interactions involved in DNA recombination and repair can be investigated.

VI. Concluding Remarks

Recent development in a single molecule imaging technique has opened a new era of molecular biology by enabling real time imaging of molecules with high spatial and temporal resolution. Especially, for the investigation of DNA damage and genome integrity, many previous "functional" discoveries have been linked to the "mechanistic" molecular details. The newly revealed molecular mechanisms highlight the extremely sophisticated molecular machines that are built to work specifically and efficiently within themselves or together with partner proteins.

While all newly emerging single molecule techniques pursue the same goal of achieving the highest molecular resolution possible, the dimensions and parameters that are tested by individual setups are diverse in nature. For example, kilobase stretches of DNA, such as λ-DNA, are used to study how the DNA repair proteins search and detect the damage site by diffusion/hopping process, while 20–50 nucleotides of ssDNA are employed to map how a protein modulates the conformation and dynamics of locally bound DNA. Some DNA repair proteins can be tagged singly to probe its motion along the DNA axis, while the same proteins can be doubly labeled to reveal its intramolecular conformational dynamics. Furthermore, DNA can be labeled at a specific site to locate a site of damage, labeled at two positions to report on its conformational dynamics induced by proteins, or a long stretch of DNA can be stained by an intercalating dye. Force can be applied to pull on DNA, or to simply hold a long stretch of DNA in place.

Another exciting development in single molecule technology is the effort being invested into combining various tools to expand measurement capability and dimension. In this paper, we discussed the combination of fluorescence and microfluidics/flow chamber, fluorescence and force, magnetic tweezers and optical trap, and fluorescence and immunofluorescence. The data depicted from each study demonstrate how one technique alone could not have reached the same depth of understanding about the individual system. We look forward to more innovations and creative tool development that will advance the current status of single molecule technology.

REFERENCES

[1] R. Kanaar, J. H. Hoeijmakers, and D. C. van Gent, "Molecular mechanisms of DNA double strand break repair," *Trends Cell Biol*., vol. 8, pp. 483–489, Dec. 1998.

[2] T. Rich, R. L. Allen, and A. H. Wyllie, "Defying death after DNA damage," *Nature*, vol. 407, pp. 777–783, Oct. 12, 2000.

[3] R. Fishel, "Signaling mismatch repair in cancer," *Nat. Med*., vol. 5, pp. 1239–1241, Nov. 1999.

[4] P. Hsieh and K. Yamane, "DNA mismatch repair: Molecular mechanism, cancer, and ageing," *Mech. Ageing Dev.*, vol. 129, pp. 391–407, Jul./Aug. 2008.

[5] C. Lengauer, K. W. Kinzler, and B. Vogelstein, "Genetic instabilities in human cancers," *Nature*, vol. 396, pp. 643–649, Dec. 17, 1998.

[6] R. D. Kolodner, C. D. Putnam, and K. Myung, "Maintenance of genome stability in saccharomyces cerevisiae," *Science*, vol. 297, pp. 552–557, Jul. 26, 2002.

[7] D. Hanahan and R. A. Weinberg, "Hallmarks of cancer: The next generation," *Cell*, vol. 144, pp. 646–674, Mar. 4, 2011.

[8] P. Modrich, "Mechanisms in eukaryotic mismatch repair," *J. Biol. Chem*., vol. 281, pp. 30305–30309, Oct. 13, 2006.

[9] J. Jiricny, "The multifaceted mismatch-repair system," *Nat. Rev. Mol. Cell Biol*., vol. 7, pp. 335–346, May 2006.

[10] T. A. Kunkel and D. A. Erie, "DNA mismatch repair," *Annu. Rev. Biochem*., vol. 74, pp. 681–710, 2005.

[11] F. Paques and J. E. Haber, "Multiple pathways of recombination induced by double-strand breaks in saccharomyces cerevisiae," *Microbiol. Mol. Biol. Rev*., vol. 63, pp. 349–404, Jun. 1999.

[12] L. S. Symington, "Role of RAD52 epistasis group genes in homologous recombination and double-strand break repair," *Microbiol. Mol. Biol. Rev.*, vol. 66, pp. 630–670, Dec. 2002.

[13] S. C. Kowalczykowski, D. A. Dixon, A. K. Eggleston, S. D. Lauder, and W. M. Rehrauer, "Biochemistry of homologous recombination in Escherichia coli," *Microbiol. Rev*., vol. 58, pp. 401–465, Sep. 1994.

[14] O. G. Berg, R. B. Winter, and P. H. von Hippel, "Diffusion-driven mechanisms of protein translocation on nucleic acids. 1. Models and theory," *Biochemistry*, vol. 20, pp. 6929–6948, Nov. 24, 1981.

[15] R. B. Winter, O. G. Berg, and P. H. von Hippel, "Diffusion-driven mechanisms of protein translocation on nucleic acids. 3. The Escherichia coli lac repressor–operator interaction: Kinetic measurements and conclusions," *Biochemistry*, vol. 20, pp. 6961–6977, Nov. 24, 1981.

[16] J. Gorman, A. Chowdhury, J. A. Surtees, J. Shimada, D. R. Reichman, E. Alani *et al*., "Dynamic basis for one-dimensional DNA scanning by the mismatch repair complex Msh2-Msh6," *Mol. Cell*, vol. 28, pp. 359–370, Nov. 9, 2007.

[17] J. Gorman, A. J. Plys, M. L. Visnapuu, E. Alani, and E. C. Greene, "Visualizing one-dimensional diffusion of eukaryotic DNA repair factors along a chromatin lattice," *Nat. Struct. Mol. Biol*., vol. 17, pp. 932–938, Aug. 2010.

[18] J. Gorman, F. Wang, S. Redding, A. J. Plys, T. Fazio, S. Wind *et al*., "Single-molecule imaging reveals target-search mechanisms during DNA mismatch repair," in *Proc. Nat. Acad. Sci. USA*, vol. 109, pp. E3074–83, Nov. 6, 2012.

[19] W. K. Cho, C. Jeong, D. Kim, M. Chang, K. M. Song, J. Hanne *et al*., "ATP alters the diffusion mechanics of MutS on mismatched DNA," *Structure*, vol. 20, pp. 1264–1274, Jul. 3, 2012.

[20] R. Qiu, V. C. DeRocco, C. Harris, A. Sharma, M. M. Hingorani, D. A. Erie *et al*., "Large conformational changes in MutS during DNA scanning, mismatch recognition and repair signalling," *EMBO J*., vol. 31, pp. 2528–2540, May 30, 2012.

[21] G. Obmolova, C. Ban, P. Hsieh, and W. Yang, "Crystal structures of mismatch repair protein MutS and its complex with a substrate DNA," *Nature*, vol. 407, pp. 703–710, Oct. 12, 2000.

[22] M. M. Cox, M. F. Goodman, K. N. Kreuzer, D. J. Sherratt, S. J. Sandler, and K. J. Marians, "The importance of repairing stalled replication forks," *Nature*, vol. 404, pp. 37–41, Mar. 2, 2000.

[23] I. De Vlaminck, M. T. van Loenhout, L. Zweifel, J. den Blanken, K. Hooning, S. Hage *et al*., "Mechanism of homology recognition in DNA recombination from dual-molecule experiments," *Mol. Cell*, vol. 46, pp. 616–624, Jun. 8, 2012.

[24] A. V. Mazin and S. C. Kowalczykowski, "The function of the secondary DNA-binding site of RecA protein during DNA strand exchange," *EMBO J*., vol. 17, pp. 1161–1168, Feb. 16, 1998.

[25] D. Sagi, T. Tlusty, and J. Stavans, "High fidelity of RecA-catalyzed recombination: A watchdog of genetic diversity," *Nucleic Acids Res*., vol. 34, pp. 5021–5031, 2006.

[26] C. M. Radding, "Helical interactions in homologous pairing and strand exchange driven by RecA protein," *J. Biol. Chem*., vol. 266, pp. 5355–5358, Mar. 25, 1991.

[27] J. H. Jeon, J. Adamcik, G. Dietler, and R. Metzler, "Supercoiling induces denaturation bubbles in circular DNA," *Phys. Rev. Lett*., vol. 105, p. 208101, Nov. 12, 2010.

[28] B. C. Wong, S. K. Chiu, and S. A. Chow, "The role of negative superhelicity and length of homology in the formation of paranemic joints promoted by RecA protein," *J. Biol. Chem*., vol. 273, pp. 12120–12127, May 15, 1998.

[29] A. L. Forget and S. C. Kowalczykowski, "Single-molecule imaging of DNA pairing by RecA reveals a three-dimensional homology search," *Nature*, vol. 482, pp. 423–427, Feb. 16, 2012.

[30] K. Ragunathan, C. Liu, and T. Ha, "RecA filament sliding on DNA facilitates homology search," *Elife*, vol. 1, p. e00067, 2012.

[31] M. Spies, "There and back again: New single-molecule insights in the motion of DNA repair proteins," *Curr. Opin. Struct. Biol*., vol. 23, pp. 154–160, Feb. 2013.

[32] T. Ha, T. Enderle, D. F. Ogletree, D. S. Chemla, P. R. Selvin, and S. Weiss, "Probing the interaction between two single molecules: Fluorescence resonance energy transfer between a single donor and a single acceptor," in *Proc. Nat. Academy Sci. USA*, Jun. 25, 1996, vol. 93, pp. 6264–6268.

[33] R. Roy, A. G. Kozlov, T. M. Lohman, and T. Ha, "SSB protein diffusion on single-stranded DNA stimulates RecA filament formation," *Nature*, vol. 461, pp. 1092–1097, Oct. 22, 2009.

[34] S. Hohng, R. B. Zhou, M. K. Nahas, J. Yu, K. Schulten, D. M. J. Lilley *et al*., "Fluorescence-force spectroscopy maps two-dimensional reaction landscape of the holliday junction," *Science*, vol. 318, pp. 279–283, Oct. 12, 2007.

[35] R. B. Zhou, A. G. Kozlov, R. Roy, J. C. Zhang, S. Korolev, T. M. Lohman *et al*., "SSB functions as a sliding platform that migrates on DNA via reptation," *Cell*, vol. 146, pp. 222–232, Jul. 22, 2011.

[36] S. V. Kuznetsov, A. G. Kozlov, T. M. Lohman, and A. Ansari, "Microsecond dynamics of protein-DNA interactions: Direct observation of the wrapping/unwrapping kinetics of single-stranded DNA around the E. coli SSB tetramer," *J. Mol. Biol*., vol. 359, pp. 55–65, May 26, 2006.

[37] R. Romer, U. Schomburg, G. Krauss, and G. Maass, "Escherichia coli single-stranded DNA binding protein is mobile on DNA: 1 H NMR study of its interaction with oligo- and polynucleotides," *Biochemistry*, vol. 23, pp. 6132–6137, Dec. 4, 1984.
[38] M. C. Murphy, I. Rasnik, W. Cheng, T. M. Lohman, and T. Ha, "Probing single-stranded DNA conformational flexibility using fluorescence spectroscopy," *Biophys. J.*, vol. 86, pp. 2530–2537, Apr. 2004.
[39] B. H. Lok and S. N. Powell, "Molecular pathways: Understanding the role of Rad52 in homologous recombination for therapeutic advancement," *Clin. Cancer Res.*, vol. 18, pp. 6400–6406, Dec. 1, 2012.
[40] M. Honda, Y. Okuno, J. Yoo, T. Ha, and M. Spies, "Tyrosine phosphorylation enhances RAD52-mediated annealing by modulating its DNA binding," *EMBO J.*, vol. 30, pp. 3368–3382, Aug. 17, 2011.
[41] H. Kitao and Z. M. Yuan, "Regulation of ionizing radiation-induced Rad52 nuclear foci formation by c-Abl-mediated phosphorylation," *J. Biol. Chem.*, vol. 277, pp. 48944–48948, Dec. 13, 2002.
[42] C. Joo, S. A. McKinney, M. Nakamura, I. Rasnik, S. Myong, and T. Ha, "Real-time observation of RecA filament dynamics with single monomer resolution," *Cell*, vol. 126, pp. 515–527, Aug. 11, 2006.
[43] S. A. McKinney, C. Joo, and T. Ha, "Analysis of single-molecule FRET trajectories using hidden Markov modeling," *Biophys. J.*, vol. 91, pp. 1941–1951, Sep. 1, 2006.
[44] M. R. Singleton, L. M. Wentzell, Y. Liu, S. C. West, and D. B. Wigley, "Structure of the single-strand annealing domain of human RAD52 protein," *Proc. Nat. Acad. Sci. USA*, vol. 99, pp. 13492–13497, Oct. 15 2002.
[45] A. Jain, R. Liu, B. Ramani, E. Arauz, Y. Ishitsuka, K. Ragunathan *et al.*, "Probing cellular protein complexes using single-molecule pull-down," *Nature*, vol. 473, pp. 484–488, May 26, 2011.
[46] J. Park, S. Myong, A. Niedziela-Majka, K. S. Lee, J. Yu, T. M. Lohman *et al.*, "PcrA helicase dismantles RecA filaments by reeling in DNA in uniform steps," *Cell*, vol. 142, pp. 544–555, Aug. 20, 2010.
[47] C. S. McHenry, "DNA replicases from a bacterial perspective," *Annu. Rev. Biochem.*, vol. 80, pp. 403–436, Jun. 7, 2011.
[48] S. Jergic, N. P. Horan, M. M. Elshenawy, C. E. Mason, T. Urathamakul, K. Ozawa *et al.*, "A direct proofreader-clamp interaction stabilizes the Pol III replicase in the polymerization mode," *EMBO J.*, vol. 32, pp. 1322–1333, May 2, 2013.
[49] N. A. Tanner, S. M. Hamdan, S. Jergic, K. V. Loscha, P. M. Schaeffer, N. E. Dixon *et al.*, "Single-molecule studies of fork dynamics in Escherichia coli DNA replication," *Nat. Struct. Mol. Biol.*, vol. 15, p. 998, Sep. 2008.
[50] N. Ribeck, D. L. Kaplan, I. Bruck, and O. A. Saleh, "DnaB helicase activity is modulated by DNA geometry and force," *Biophys. J.*, vol. 99, pp. 2170–2179, Oct. 6, 2010.
[51] S. Jergic, K. Ozawa, N. K. Williams, X. C. Su, D. D. Scott, S. M. Hamdan *et al.*, "The unstructured C-terminus of the tau subunit of Escherichia coli DNA polymerase III holoenzyme is the site of interaction with the alpha subunit," *Nucleic. Acids Res.*, vol. 35, pp. 2813–2824, 2007.

Sua Myong received the B.S. degrees in molecular and cellular biology and the Ph.D. degree in nutritional sciences, all from the University of California, Berkeley, CA, USA. She received her postdoctoral training in the laboratory of Taekjip Ha, Department of Physics, University of Illinois, Urbana, IL, USA, where she developed her skills in molecular biology and single molecule biophysics experiments. In the Ha lab, she participated in the discovery of molecular mechanisms of DNA and RNA motor proteins which have been published in *Science*, *Nature*, *and Cell*. She was an Assistant Professor in the Department of Bioengineering, University of Illinois in 2009.

Her research interest include study of nucleic acid–protein interactions that are involved in the Central dogma of biology and pathways relevant to human diseases. The Myong lab is engaged in research related to DNA recombination/repair, RNA interference, telomere processing, Ribonucleoprotein assembly and dynamics.

Dr. Myong received the American Cancer Society Research Award (2010), Human Frontier Science Program Award (2011), and the NIH New Director's Innovator Award (2012). In 2010, she was also named Genome Technology's annual list of "Tomorrow's PIs" for her contribution in single molecule research.

Yupeng Qiu received the B.S. degrees in biomedical engineering and electrical engineering from Duke University, Durham, NC, USA, in 2006 and the M.S. degree in bioengineering from the University of Illinois at Urbana-Champaign, Urbana, IL, USA, in 2009, where she is currently working toward the Ph.D. degree in bioengineering.

Her research interests include using single molecule FRET and PIFE techniques to study proteins involved in DNA recombination. Ms. Qiu is a current member of the Biophysical Society.